Protection of CTR Metallic First Walls by Neutron Spectral Shifting – Preliminary Draft

G.L. Kulcinski, R.W. Conn, H.I. Avci, and D.K. Sze

June 3, 1975

UWFDM-127

FUSION TECHNOLOGY INSTITUTE

UNIVERSITY OF WISCONSIN

MADISON WISCONSIN

Protection of CTR Metallic First Walls by Neutron Spectral Shifting – Preliminary Draft

G.L. Kulcinski, R.W. Conn, H.I. Avci, and D.K. Sze

Fusion Technology Institute
University of Wisconsin
1500 Engineering Drive
Madison, WI 53706

http://fti.neep.wisc.edu

June 3, 1975

UWFDM-127

Protection of CTR Metallic First Walls by Neutron Spectral Shifting

by

Gerald L. Kulcinski

Robert W. Conn

Halil I. Avci

Dai Kai Sze

June 3, 1975

FDM-127

Nuclear Engineering Dept.
University of Wisconsin
Madison, Wisconsin 53706

Introduction

The use of passive carbon shields to protect the plasma and the metallic first walls of a fusion reactor has been recently proposed.[1,2] Carbon curtains were shown to considerably reduce the plasma energy losses due to impurity atom build-up, while at the same time protecting the first wall from erosion due to plasma ion induced blistering and sputtering. It was also shown that increasing the thickness of the curtain degrades the neutron spectrum sufficiently such that displacement damage, gas production rates and long term radioactivity is reduced in vanadium. This concept was given the acronym ISSEC, for Internal Spectral Shifter and Energy Convertor.[2]

The purpose of this paper is to expand the ISSEC concept to other materials and to more fully address the temperature limitations of the passive carbon shifter. We will not discuss the concepts of internal tritium breeding and neutron absorption as these are treated elsewhere.[2]

II. Calculational Procedures

The one dimensional-homogeneous blanket design used for this work is shown in figure 1. A variable thickness carbon zone was placed between a D-T plasma and the first wall. A density factor (D.F.) of 1.0 was used for the neutronic calculations although in practice a D.F. of ~0.7 would be more reasonable and would result in a thicker ISSEC region. However the neutron 'optical' thickness would be the same in both cases. The first wall thickness of 1 cm at a D.F. of 1.0 is intended to cover most reactor design cases. Again, lower D.F.'s and increased thicknesses would be used in practice to include coolant (which we assumed to be helium gas) and void spaces. The first wall is followed by a 60 cm thick reflector-shield region composed of 30% B_4C (enriched to 90% B-10) and 70% carbon. An albedo of 0.2 was used to simulate the final shield for the first five neutron energy groups (9 to 14.9 MeV)

and an albedo of 0.3 was used for neutrons of lower energy. Obviously, no attempt was made to breed tritium in this reactor design but only to highlight the anticipated structural materials responses to the degraded neutron spectra.

The nuclear performance of this type of reactor design was studied by solving the discrete ordinates form of the neutron transport equation using the ANISN[3] program with a S_4-P_3 approximation. It has been shown elsewhere[4] that this approximation is adequate to predict integral parameters such as tritium breeding and gas production rates to within approximately 2% of a higher order calculation like the S_{16}-P_5. The neutron multigroup cross sections (except for gas production in molybdenum) were processed using the program SUPERTOG[5] from nuclear data in ENDF/B3.[6] Gas production cross sections for Mo were calculated by Pearlstein.[7] The displacement cross sections were calculated from a computer code developed by Doran[8,9] and the values used in these calculations are given in Appendix A. All calculations were performed using 46 energy groups.

The reactions considered for the radioactivity calculations, along with appropriate branching ratios and half lives are given in Appendix B. The radioactivity and appropriate decay factors for 316 SS were calculated using a special computer program developed at the University of Wisconsin.[10] The composition of 316 SS was assumed to be 70% Fe, 18% Cr and 12% Ni for all calculations except radioactivities. The composition used for the 316 SS is given in Appendix C. Such a detailed procedure was necessary because of the complex nature of the 316 SS alloy and the large number of primary and secondary reactions that could take place.

The heat transfer calculations in the carbon ISSEC were accomplished by assuming solid material with an average heat transfer coefficient of 0.42 watt

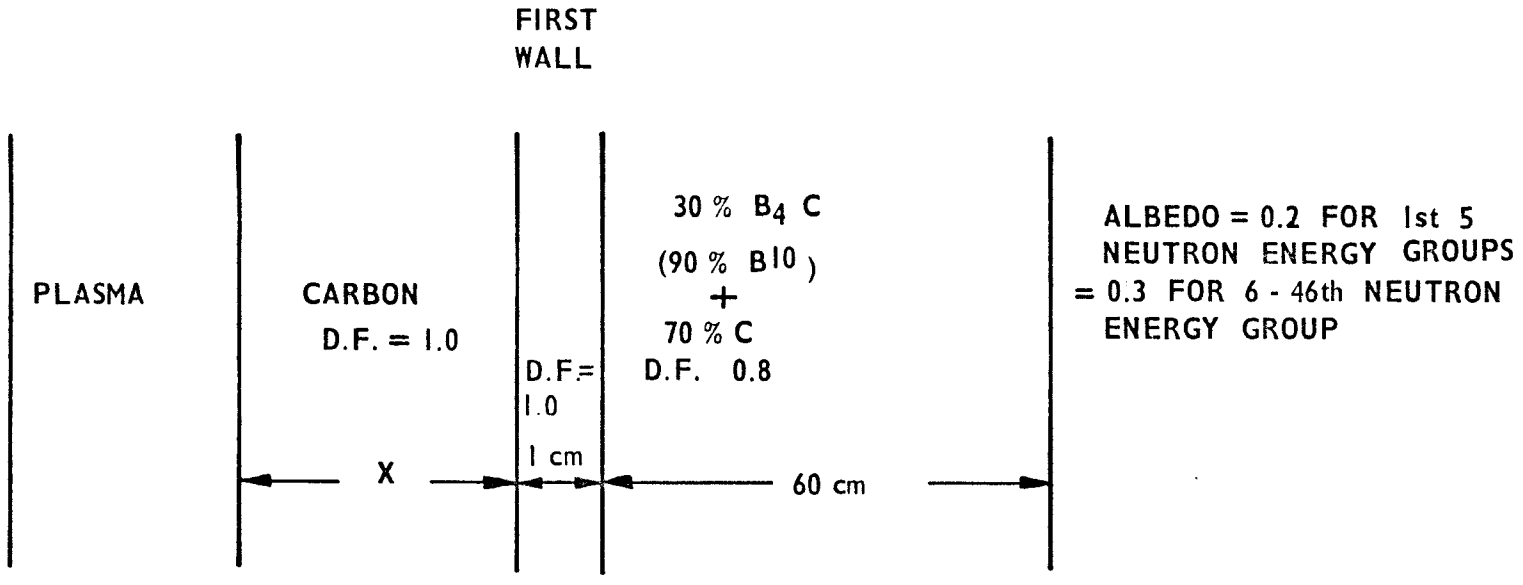

D.F. = DENSITY FACTOR.

FIG. 1 MODEL BLANKET DESIGN USED TO STUDY THE EFFECT OF GRAPHITE SPECTRAL SHIFTER ON THE RADIATION DAMAGE PARAMETERS IN THE FIRST WALL.

$cm^{-1}°C^{-1}$ (assumed to be constant over a 1200-2000°C temperature span). The metallic first wall temperature was assumed to be 800°C for this work although in practice this would be less for 316 SS and Al. A reduction in this temperature would slightly lower the temperature in the ISSEC due to increased radiative heat transfer. A surface heat flux of 10 watts/cm^2 was assumed in all cases. In the case of a partial ISSEC, the carbon curtain temperature was calculated to be in the range of 1200-1300°C.

III. Irradiation Environments Inside Carbon ISSEC's

A.) Temperature considerations

The slowing down of neutrons in carbon ISSEC's results in high nuclear heating values (~1-6 watts per cm^3 per MW/m^2). These volumetric heating rates, coupled with high surface heat loadings, will produce very high temperatures in a passive carbon shield which is constrained to transfer heat by radiative mechanisms. A detailed analysis of the temperature distributions in full and partial ISSEC's is given elsewhere[11] and only a few comments will be made here.

The main factor limiting the use of an ISSEC is the maximum surface temperature it can sustain without an excessive vapor pressure. We have chosen a maximum vapor pressure of 10^{-5} torr for this work. Such a vapor pressure would roughly approximate the background pressure in an operating tokamak. The limit of 10^{-5} torr imposes a maximum temperature of ~2000°C on the carbon and this temperature limit, coupled with the neutron wall loading, will determine the ultimate thickness (and usefulness) of the carbon zone. An example of this limitation is shown in figure 2 where the maximum surface temperature (facing the plasma) for a full ISSEC is plotted as a function of carbon thickness. This figure shows that the maximum ISSEC thickness for a 1 MW/m^2 neutron wall loading is ~6.5 cm of 100% D.F. carbon. This drops to 3.3 cm at a 2 MW/m^2 wall loading.

Figure 2 also shows that the situation changes significantly for partial ISSEC's where the maximum surface and maximum inner temperatures are plotted as a function of carbon thickness. Here one can see that at 1 MW/m^2, partial ISSEC's of 25-30 cm thickness could be used without T_{max}^{inner} exceeding 2000°C. It is also found that if it is the surface, and not the inner temperature, which determines the useful thickness, then essentially infinite thicknesses can be used. If the wall loading is increased to 2 MW/m^2 and the T_{max}^{inner} limit is used, a 12 cm

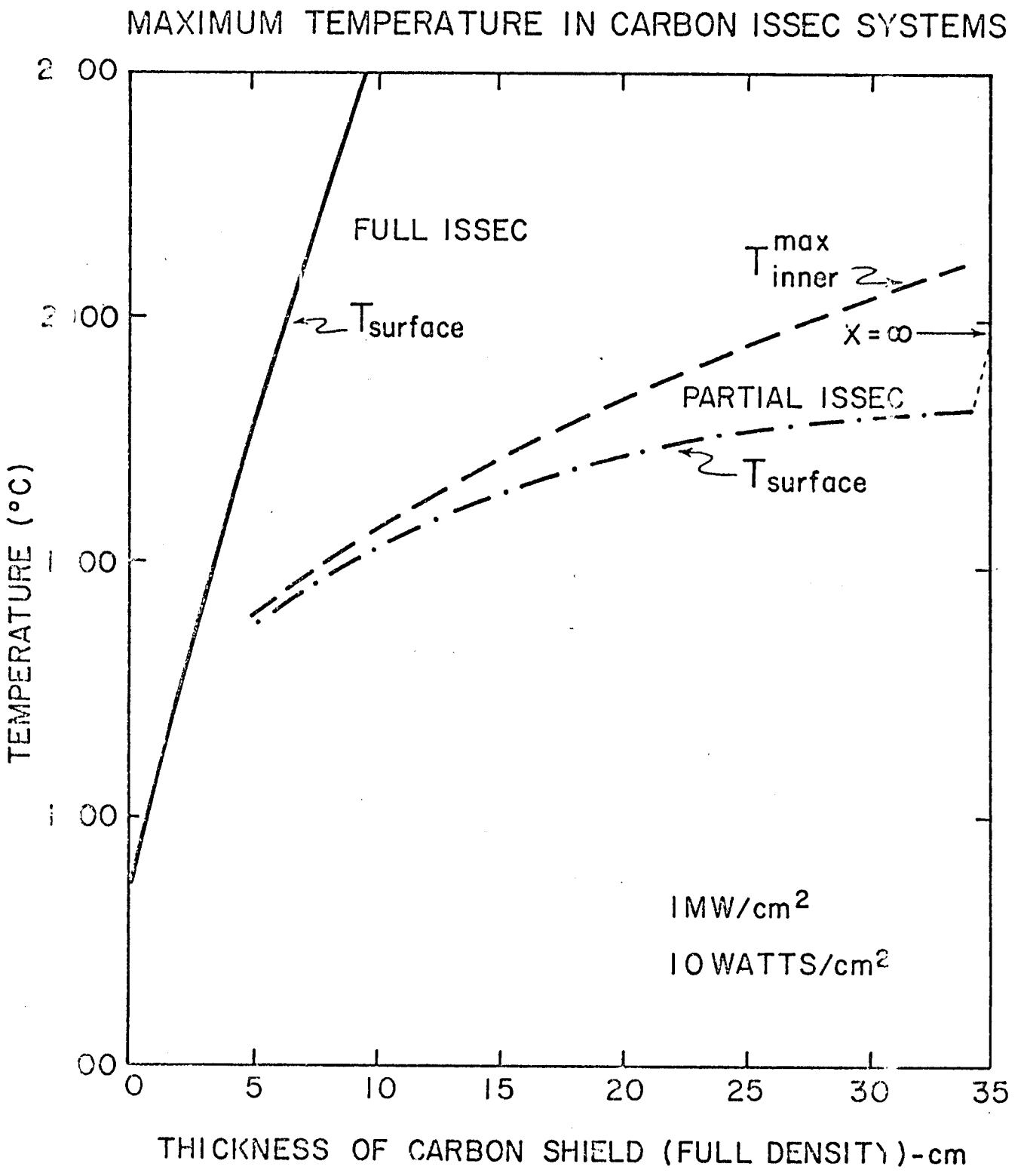
MAXIMUM TEMPERATURE IN CARBON ISSEC SYSTEMS
2 00
2 00
1 00
1 00
00
TEMPERATURE (°C)
FULL ISSEC
T surface
T max inner
X = ∞
PARTIAL ISSEC
T surface
1MW/cm2
10WATTS/cm2
0
5
10
15
20
25
30
35
THICKNESS OF CARBON SHIELD (FULL DENSITY)-cm

FIGURE 2

thickness is allowed while thickness of ~50 cm could be used if the surface temperature is limiting.

It is obvious from the above considerations that carbon ISSEC thicknesses of as little as 6 cm to infinite values could be used as passive shields for nominal CTR neutron wall loadings. Subsequent analysis will now be performed only as a function of carbon thickness and no specific reference will be made to full or partial ISSEC's.

B.) Radiation Damage Considerations Within Carbon ISSEC's

The slowing down of neutrons in the carbon results from three main mechanisms

- elastic neutron scattering
- inelastic neutron scattering
- (n,n') $3He^4$ reactions.

All three result in displaced atoms while the latter reaction tends to produce a large amount of helium gas. Figure 3 shows how the displacement damage normalized to a 1 MW/m^2 wall loading varies inside of a carbon ISSEC. The displacement cross sections of Morgan[12] were used. The temperature distribution for a 6 cm thick-full ISSEC and a 30 cm thick partial ISSEC, both at 1 MW/m^2 wall loading, is also shown. The major point to draw from this figure is that most of the displacement damage in ISSEC systems will occur in carbon at or above 1200°C. Previous analyses[13] of the dimensional instabilities of various forms of carbon reveal that displacement values of up to ~10 dpa can be accumulated at temperatures below 1200°C without excessive swelling. This would predict a one year lifetime at 1 MW/m^2. At higher temperatures the allowable damage levels are expected to be even higher and lifetimes longer.

The effect of high helium contents has not been thoroughly investigated but recent experiments by Bauer et al.[14] give some reason to hope that little permanent damage will be done. They found that the reemission rate of helium

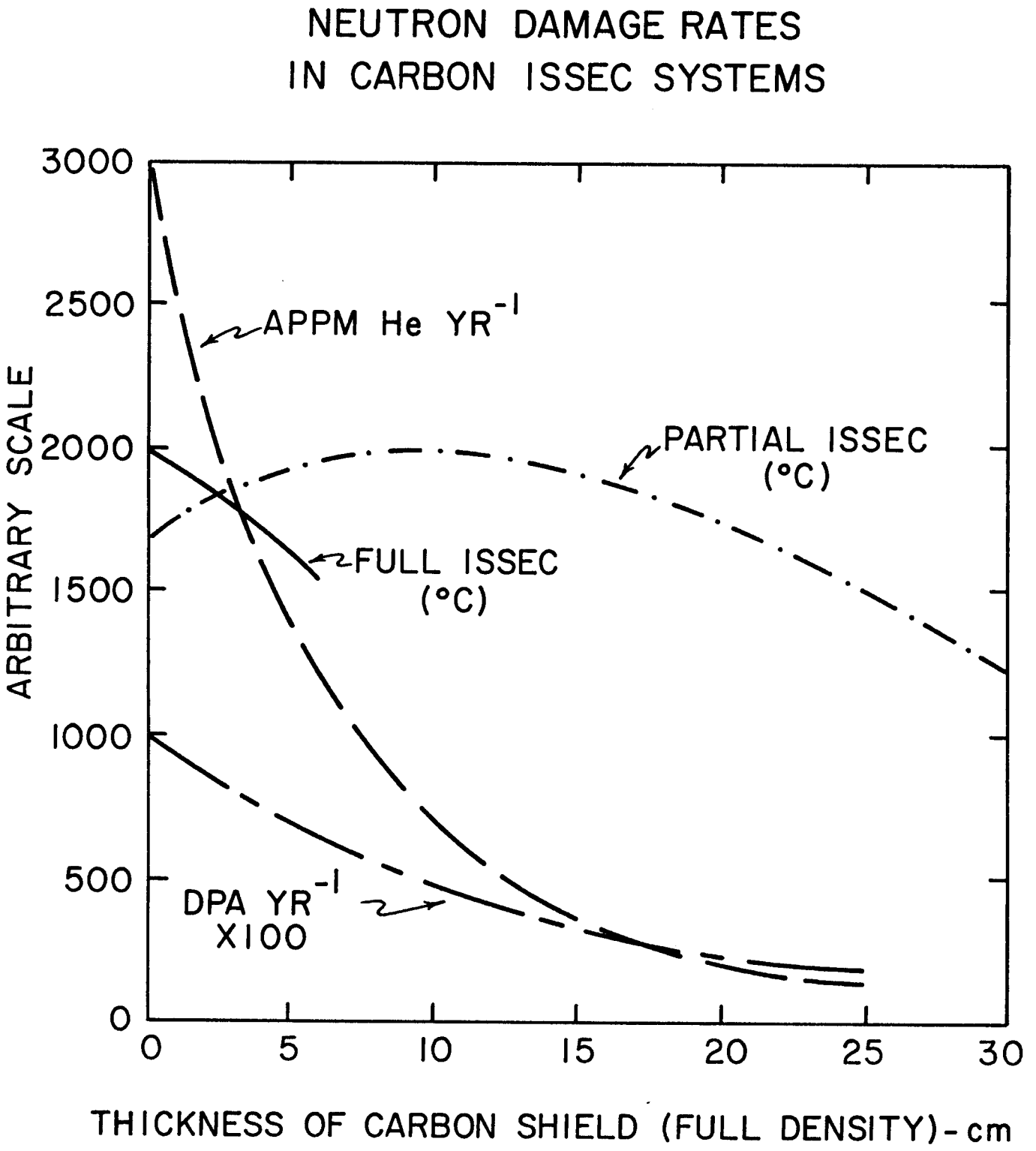
NEUTRON DAMAGE RATES
IN CARBON ISSEC SYSTEMS
3000
2500
2000
1500
1000
500
0
ARBITRARY SCALE
APPM He YR-1
PARTIAL ISSEC
(°C)
FULL ISSEC
(°C)
DPA YR-1
X100
0
5
10
15
20
25
30
THICKNESS OF CARBON SHIELD (FULL DENSITY)-cm

FIGURE 3

bombarded carbon was very high (essentially 100%) at temperatures of 1200°C. If this holds true for the carbon in an ISSEC, then perhaps there is little cause for concern about the several thousand appm of helium gas that will be generated per year of operation at 1 MW/m^2. More work is needed to verify this assumption.

IV. Reduction of Displacement Damage in Potential CTR Materials

Typical first wall neutron spectra for 0 and 12.5 cm of carbon thickness are given in Appendix D for Ta and 316 SS first walls. The combination of such neutron spectra with displacement cross sections in Appendix A yield the displacement rates listed in Table 1 and displayed in Figure 4.

The reader should be cautioned that it is the relative and not absolute rates of damage which are important. This is because one cannot accurately compare one element with another on dpa values alone; the homologous temperature of irradiation has as much or more influence on the final damage state as does the total damage level.

A few interesting observations can be made from Table I. In general, the effectiveness of the carbon ISSEC in reducing the total dpa level increases with atomic number. This is due to the increased anisotropy of neutron scattering in low Z elements which in turn tends to reduce the average energy of the PKA's. A softening of the neutron spectra then has less of an effect on low Z than it does for high Z elements. Another factor is the increased amount of damage energy available in high Z elements. This is due to the higher energy required for ionization losses in high Z metals.

It should be noted here that the displacement cross sections treat charged particle-out reactions [(n,p)(n,α) etc.] as (n,n') reactions. Recent analyses show that this underestimates the damage done by higher energy neutrons by the following factors[15]

	% underestimate at 14 MeV
Al	16
V	5
316 SS	17
Nb	3
Mo	No data
Ta	0.06

Table 1

Effect of Carbon ISSEC on Displacement Damage in Various CTR Materials

Material	dpa/year[a]		Reduction Factor
	No ISSEC	12.5 cm C	
Al	12.7	3.4	0.27
V	12.9	3.80	0.29
316 SS	11.3	2.50	0.22
Nb	8.48	1.64	0.19
Mo	9.47	1.77	0.19
Ta	8.42	1.60	0.19

[a] 1 MW/m^2, 100% Duty Factor.

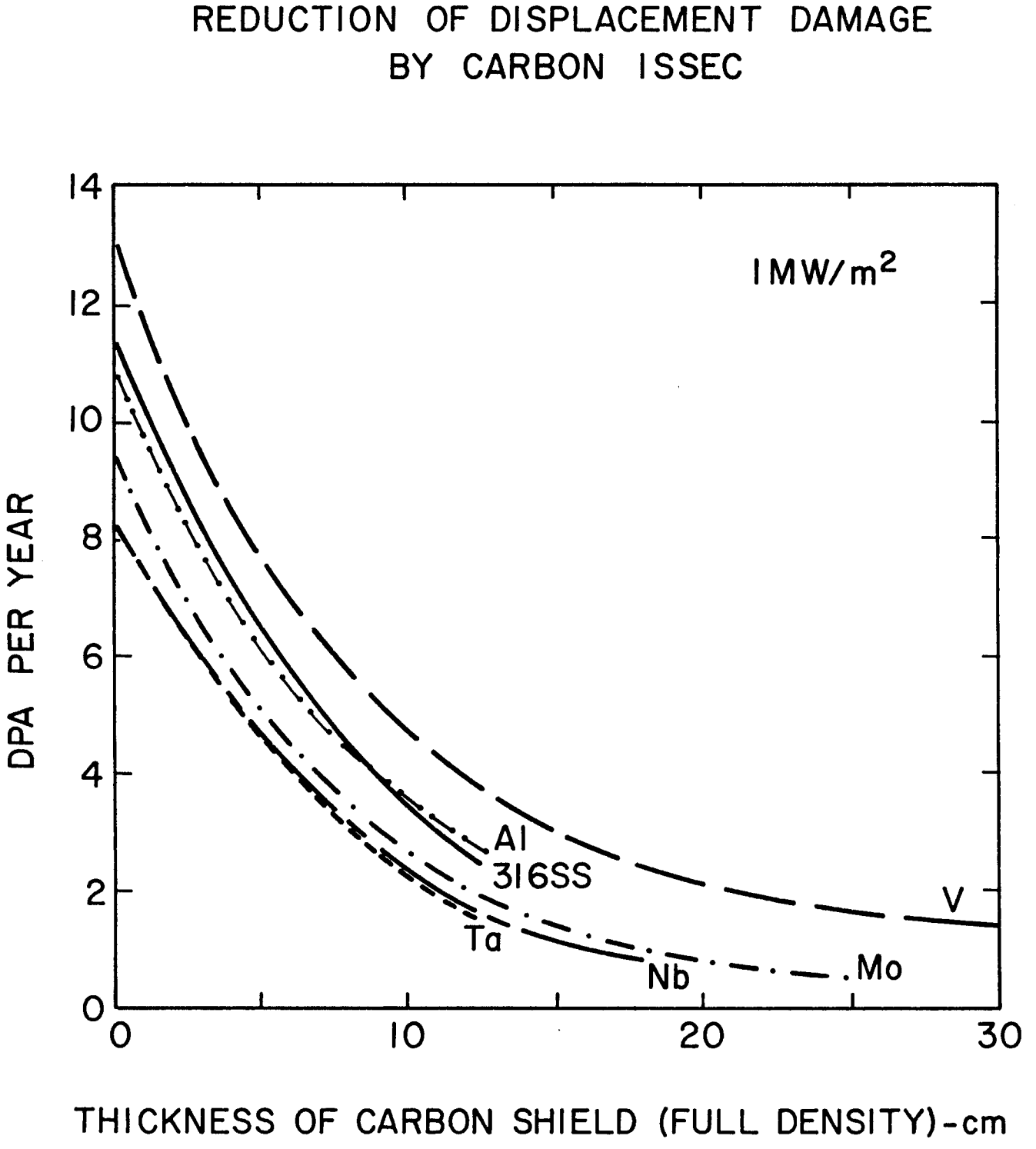
REDUCTION OF DISPLACEMENT DAMAGE
BY CARBON ISSEC
1MW/m²
DPA PER YEAR
THICKNESS OF CARBON SHIELD (FULL DENSITY)-cm
Al
316SS
Ta
Nb
Mo
V
0
2
4
6
8
10
12
14
0
10
20
30

FIGURE 4

The inclusion of these contributions would increase the dpa level in the case of no ISSEC, but would have little effect on the dpa values in ISSEC protected systems. It is therefore concluded that even including these correction factors, there still would be a slight advantage to using ISSEC's with high Z as compared to low Z elements.

Turning to the relative reduction as a function of carbon thickness, we see in Figure 5 that reduction by a factor of 3-5 can be achieved using 12.5 cm of carbon while reductions by a factor of 20 can be accomplished by using 25 cm of carbon ISSEC in front of Mo. The significance of this observation is that if the wall life is predominately determined by the level of the total displacement damage (without regard to the spatial configuration of defects) then one might extend wall lifetime due to radiation damage alone by factors of 3-20.

V. Reduction of He and H Production Rates

Table 2 lists the effect of carbon ISSEC thickness on the reduction of helium and hydrogen gas production rates (See also Figure 6). The absolute effect here is much more pronounced than in the case of displacement damage. Reductions in helium gas production range from 7-14 for 12.5 cm of carbon and from 7-11 for hydrogen production with the same carbon thickness. Except for V and Al, the reduction in He production is always greater than that for the reduction in hydrogen production. The reduction in helium gas production in Ta is a factor of 2 more than the reduction in V. This is due to the lower threshold for (n,α) reactions in V (~7 MeV) than for Ta (11 MeV).

The relative reduction values are plotted in Figure 7 and it is to be noted that on a linear scale there is little difference between the elements. If there is a discernable trend, it is that the relative reduction is greater for high Z elements than for low Z elements. This is undoubtedly due to the higher coulomb barrier (and therefore higher threshold energies) for (n,α) reactions in the high Z elements.

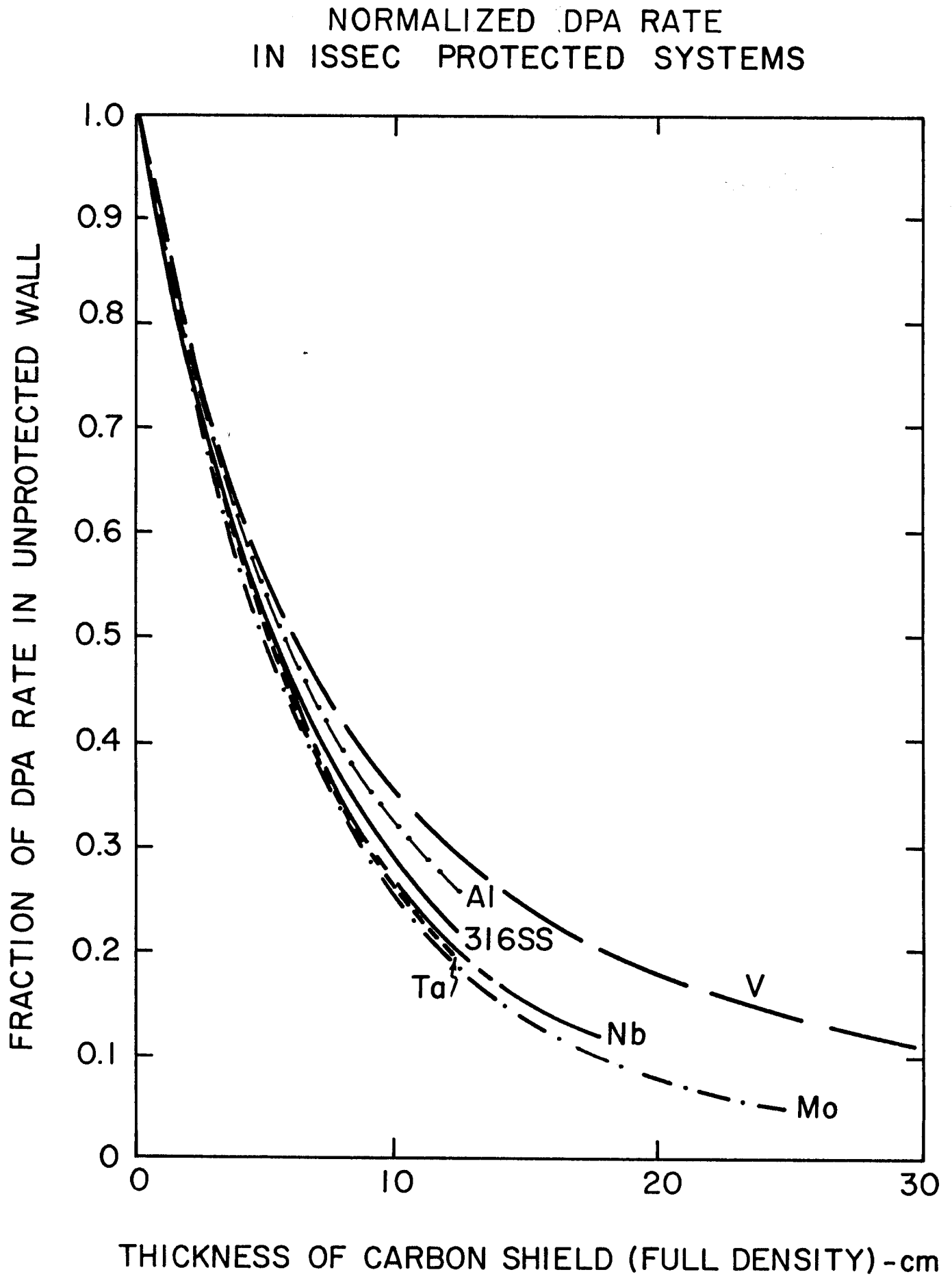
NORMALIZED DPA RATE
IN ISSEC PROTECTED SYSTEMS
FRACTION OF DPA RATE IN UNPROTECTED WALL
1.0
0.9
0.8
0.7
0.6
0.5
0.4
0.3
0.2
0.1
0
0
10
20
30
THICKNESS OF CARBON SHIELD (FULL DENSITY) - cm
Al
316SS
Ta
V
Nb
Mo

FIGURE 5

Table 2

Effect of Carbon ISSEC Thickness on the Gas Production Rates in Potential CTR Materials[(a)]

Material	appm He/yr No ISSEC	12.5 cm ISSEC	Reduction Factor	appm H/year No ISSEC	12.5 cm ISSEC	Reduction Factor
Al	476	50.1	0.11	1110	111	0.10
V	78.6	11.4	0.15	143	28.6	0.20
316 SS	280	26.8	0.10	736	100	0.14
Nb	32.7	3.32	0.10	110	12.6	0.11
Mo	72.6	6.95	0.10	149	13.7	0.09
Ta	7.52	0.55	0.07	0	0	-

(a) 1 MW/m^2, 100% Duty Factor

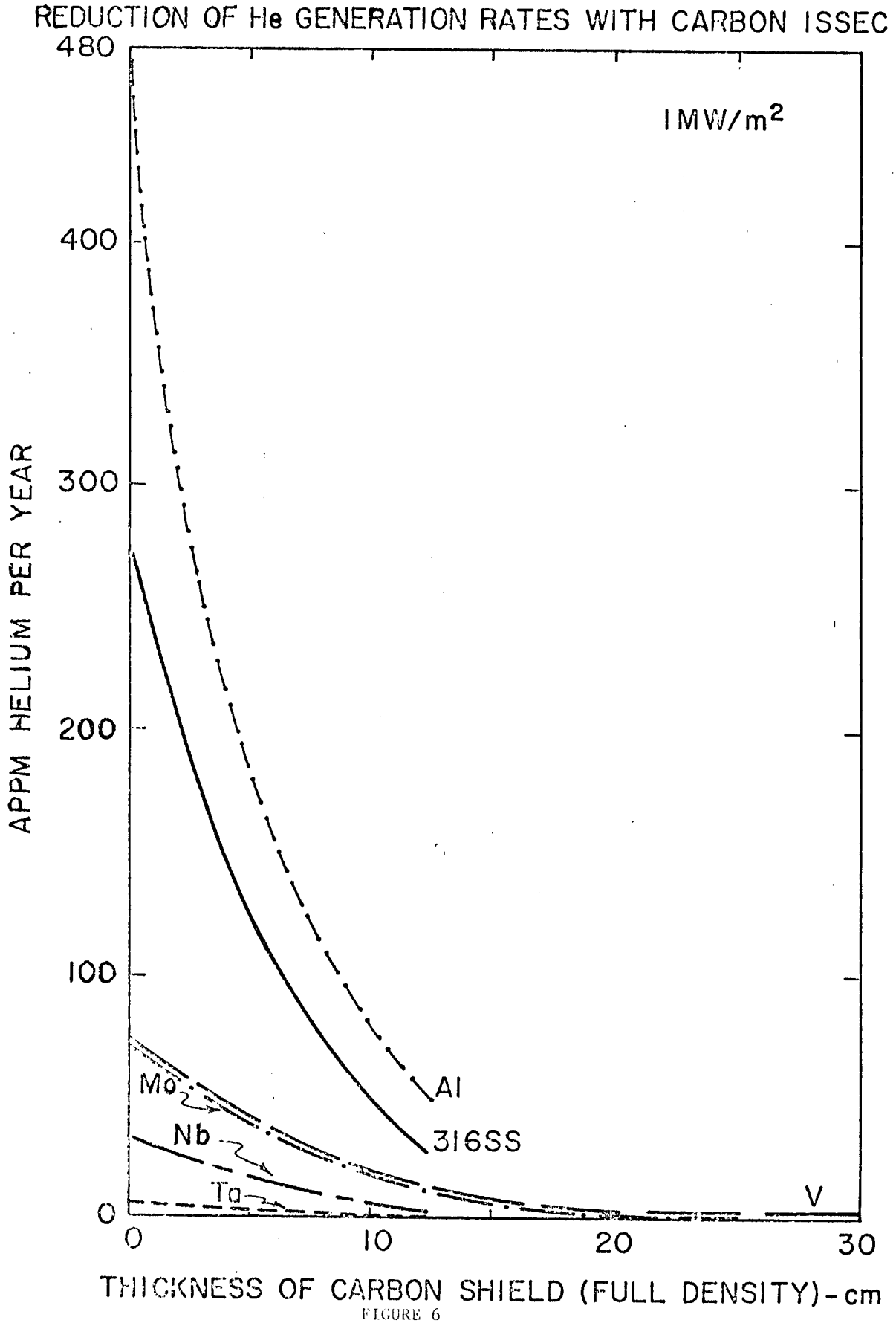
REDUCTION OF He GENERATION RATES WITH CARBON ISSEC
480
400
300
200
100
0
APPM HELIUM PER YEAR
1MW/m2
Al
316SS
Mo
Nb
Ta
V
0
10
20
30
THICKNESS OF CARBON SHIELD (FULL DENSITY)-cm

FIGURE 6

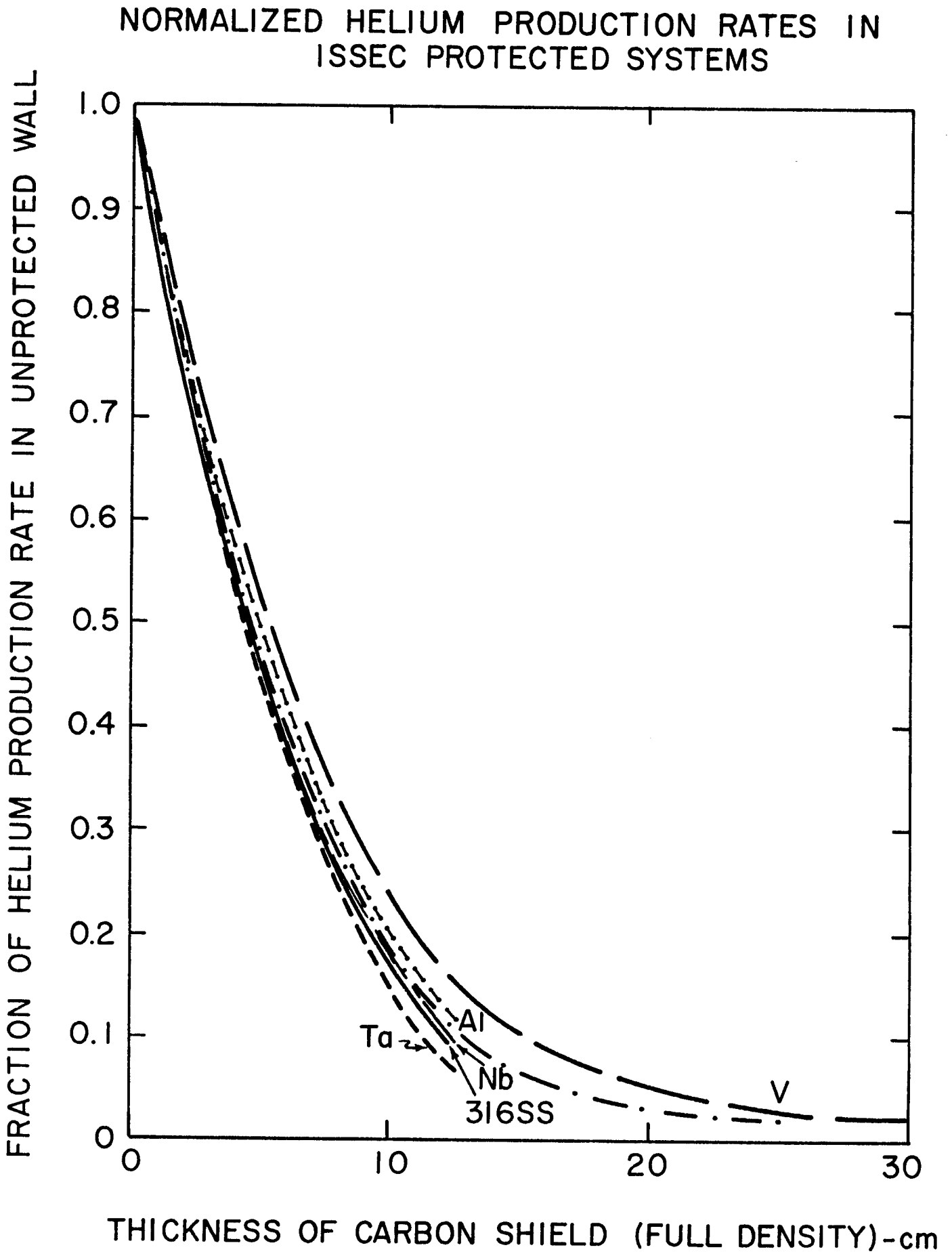
NORMALIZED HELIUM PRODUCTION RATES IN ISSEC PROTECTED SYSTEMS
FRACTION OF HELIUM PRODUCTION RATE IN UNPROTECTED WALL
1.0
0.9
0.8
0.7
0.6
0.5
0.4
0.3
0.2
0.1
0
0
10
20
30
THICKNESS OF CARBON SHIELD (FULL DENSITY)-cm
Ta
Al
Nb
316SS
V

FIGURE 7

VI. Effect of ISSEC's on the Neutron Induced Radioactivity

There are two ways to look at this effect. First, there is the change in total activity at reactor shutdown (regardless of isotope half life). Secondly, one could consider the change in only the long lived isotopes. The results of the present calculations are summarized for both time frames in Tables 3 and 4 and displayed in Figures 8 and 9.

It can be seen from Figure 8 that the use of an ISSEC can both decrease and increase the induced radioactivity. This can be understood if the element has a large activation cross section for thermal neutrons. Such is the case for V-52 ($t_{1/2}$ = 3.75 m) and Ta^{-182}($t_{1/2}$ = 115 d). The largest reduction of radioactivity at shut down is in 316 SS (a factor of 6 for 12.5 cm of carbon). This reduction is due to the effect of a softer neutron spectra on Mn-56 ($t_{1/2}$ = 2.58 h) and Fe-55 ($t_{1/2}$ = 2.7 years).

The reduction of long term activity ($t_{1/2}$ > 1 year) is even greater for 316 SS and Al than for the change in short term activity. On the other hand, the increase, in long term radioactivity for Nb and Ta is also greater. V decays to insignificant levels ($<10^{-15}$ curies/cm^3) after 1 year so that no meaningful comparison can be made at that time. However, if we examine the activity 1 week after shutdown, we find that 12.5 cm of carbon significantly reduces that radioactivity in V (to 15% of that for unprotected wall). A summary of the isotopes responsible for these effects is given in Table 5.

Discussion

It is clear from the present work that the use of carbon ISSEC's can significantly reduce the damage rates in potential CTR materials whether measured as a function of total displacement damage or as a function of gas production rates. Another way to look at this benefit is to examine the ratio

Table 3

Level of Neutron Induced Radioactivity at Shutdown in First Wall of an ISSEC Protected System[a]

Material	curies/cm^3 No ISSEC	curies/cm^3 12.5 cm ISSEC	Fraction of Unprotected First Wall Values
Al	47.4	20.4	0.43 (decrease)
V	13.3	32.8	2.44 (increase)
316 SS	91.2	15.3	0.17 (decrease)
Nb	138	60.4	0.43 (decrease)
Mo	NA	NA	NA
Ta	471	925	1.96 (increase)

[a] Two years of Irradiation

NA - Not Available

Table 4

Level of Neutron Induced Radioactivity 1 Year After Shutdown in the First Wall of ISSEC Protected[a]

Material	curies/cm^3 No ISSEC	curies/cm^3 12.5 cm of ISSEC	Fraction of Unprotected First Wall Values
Al	1.49×10^{-5}	9.14×10^{-7}	.06 (decrease)
V	$<10^{-15}$	$<10^{-15}$	0.15[b] (decrease)
316 SS	27.4	3.6	0.13 (decrease)
Nb	0.001	0.0038	3.85 (increase)
Mo	NA	NA	NA
Ta	8.22	65.6	8 (increase)

NA - Not Available

[a] After 2 years of Irradiation

[b] Value 1 week after shutdown

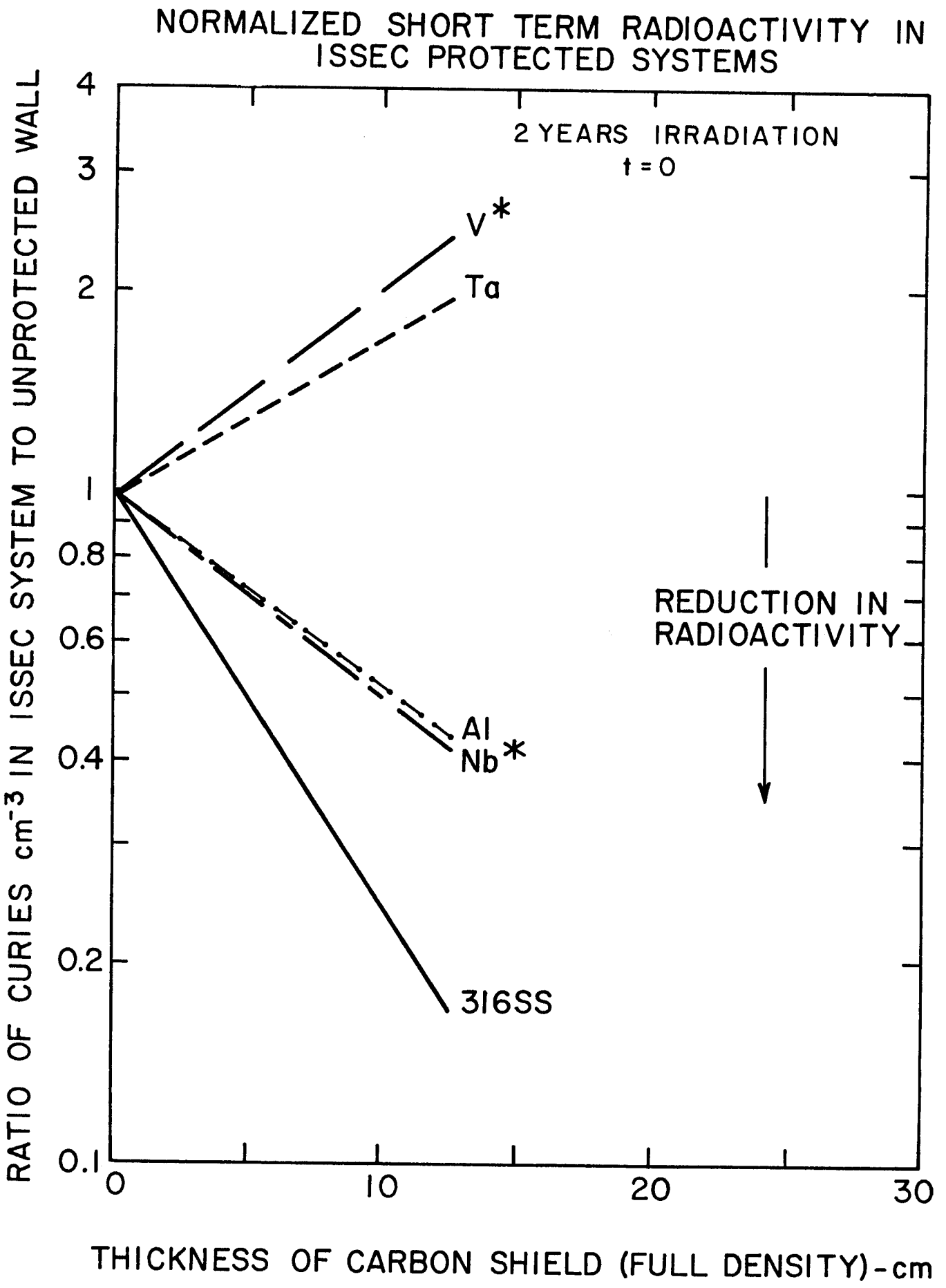
NORMALIZED SHORT TERM RADIOACTIVITY IN ISSEC PROTECTED SYSTEMS
2 YEARS IRRADIATION
t = 0
V*
Ta
Al
Nb*
316SS
REDUCTION IN RADIOACTIVITY
RATIO OF CURIES cm-3 IN ISSEC SYSTEM TO UNPROTECTED WALL
4
3
2
1
0.8
0.6
0.4
0.2
0.1
0
10
20
30
THICKNESS OF CARBON SHIELD (FULL DENSITY)-cm

FIGURE 8

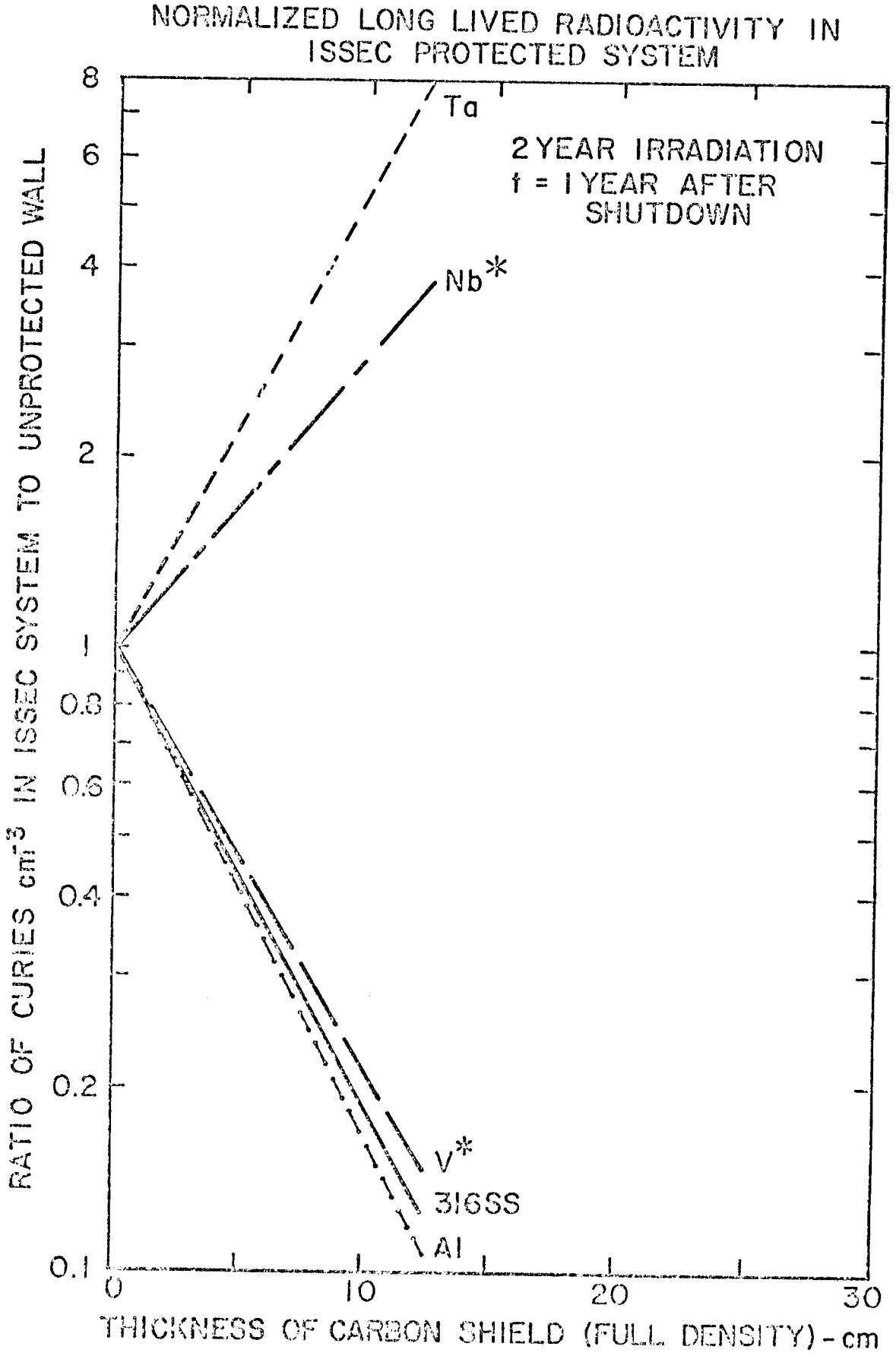
NORMALIZED LONG LIVED RADIOACTIVITY IN ISSEC PROTECTED SYSTEM
2 YEAR IRRADIATION
t = 1 YEAR AFTER SHUTDOWN
Ta
Nb*
V*
316SS
Al
RATIO OF CURIES cm⁻³ IN ISSEC SYSTEM TO UNPROTECTED WALL
8
6
4
2
1
0.8
0.6
0.4
0.2
0.1
0
10
20
30
THICKNESS OF CARBON SHIELD (FULL DENSITY) - cm

Figure 9

Table 5

Summary of Major Isotopes that Contribute to Change in Radioactivity of ISSEC Protected Systems

Material	Effect on Short Term Radioactivity	Major Isotope(s) Effected	Half Life	Effect on Long Term Radioactivity	Major Isotope Effected	Half Life
Nb	decrease	Nb-92m	10.13 d	increase	Nb-94	2.0×10^4 y
V	increase	V-52	3.75 m	decrease[a]	Sc-48	1.82 d
316 SS	decrease	Mn-56 Fe-55	2.58 h 2.7 y	decrease	Fe-55	2.7y
Al	decrease	Na-24 Mg-27	15 h 9.5 m	decrease	Al-26	7.4×10^5 y
Ta	increase	Ta-182	115 d	increase	Ta-182	115 d

[a] Consideration of intermediate term radioactivity

of the gas production rate to the displacement rate. Table 6 lists the calculated appm He to dpa ratios for the five elements and one alloy considered here. It is found this ratio varies from 1-44 for unprotected walls. Appropriate values for a fast reactor (EBR-II) and a thermal reactor (HFIR) test facility are also included in Table 6.[13] These latter values vary from 0.006-0.31 for most elements with 316 SS having a value of 95 in HFIR because of the Ni-58 to Ni-59 conversion and subsequent high thermal neutron (n,α) cross sections.

The effect of increasing the carbon ISSEC thickness on this ratio is also given in Table 6 and displayed in Figure 10. The general trend is to reduce the gas to dpa ratio by a factor of 2-3 with a 12.5 cm carbon thickness. However, the reduction still leaves the gas to dpa ratio far greater than that in current fission reactor test facilities. This is amply demonstrated in Figures 11 and 12 where the values of (appm He/dpa) for ISSEC systems are divided by those in EBR-II and HFIR, respectively. The important point to note here is that even behind ~30 cm of a carbon ISSEC the (gas/dpa) ratio is still ~40-300 times higher than for EBR-II reactors and a factor of 20-200 higher than for HFIR. The lower values tend to be for the higher Z elements.

The significance of this comparison is that while the ISSEC's can significantly reduce the absolute dpa and gas production rates, any process that depends on the <u>interaction</u> of gas atoms and point defects will not be the same in fusion reactors as found in fission reactors. Such a conclusion does not hold for PKA spectra as has been previously discussed.[2]

It appears that the reduction in short activity can be quite substantial in Al, Nb and 316 SS systems. This also means that the afterheat generated immediately after shutdown of the reactor can be considerably less. Another advantage is the reduced potential for the release of radioisotopes in the

Table 6

Calculated Ratio of appm He Gas Production To
Displaced Atom Density

	appm He/dpa				
Material	No ISSEC	12.5 cm ISSEC	25 cm ISSEC	EBR II	HFIR
Al	37.5	14.7		0.10	0.31
V	6.1	3.0		0.0057	0.0094
316 SS	24.8	10.7		0.11	95[a]
Nb	3.9	2.0		0.034	0.073
Mo	7.7	3.9	2.8	0.059	0.12
Ta	0.89	0.34		NA	NA

(a) After 1 year of irradiation

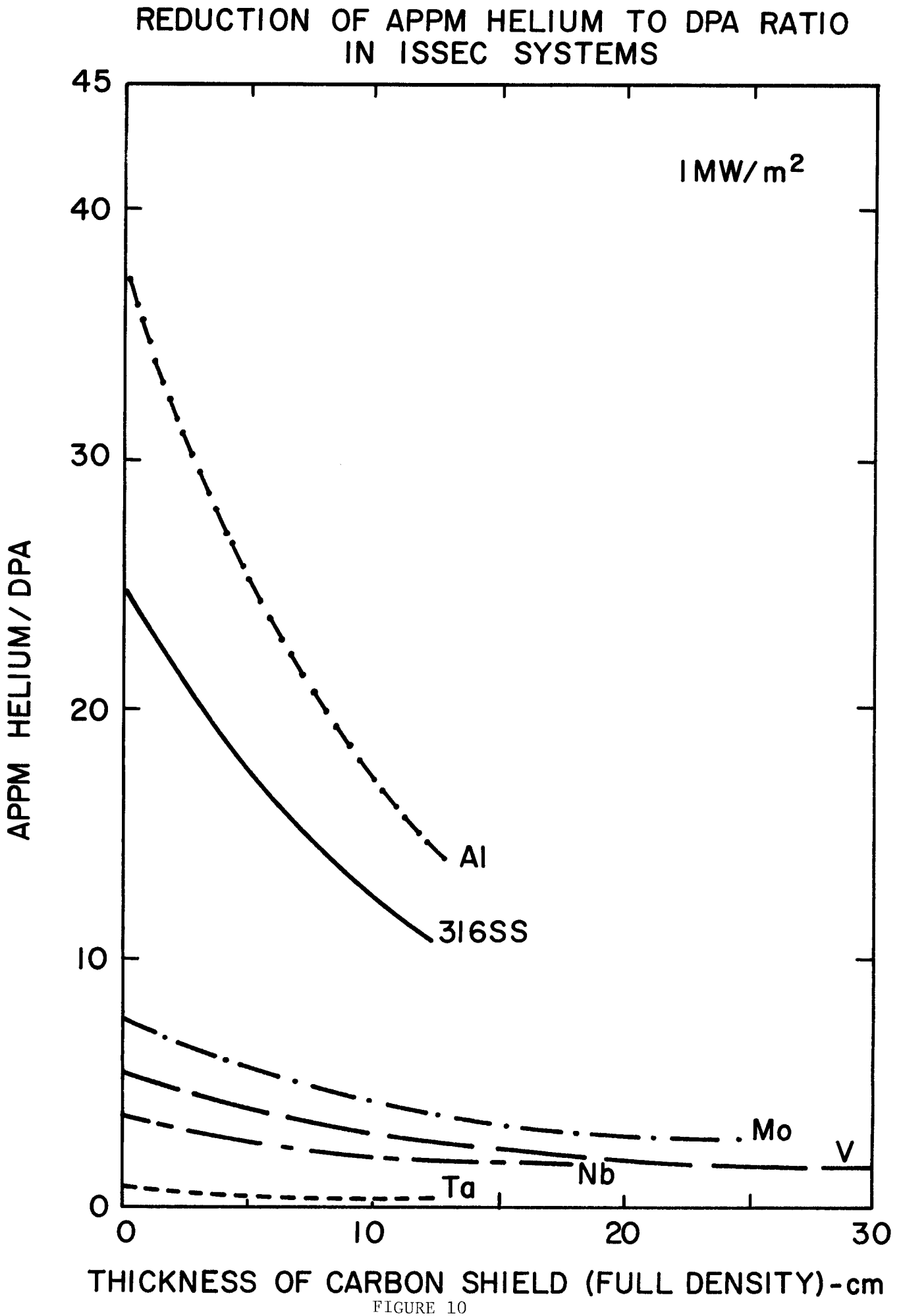
REDUCTION OF APPM HELIUM TO DPA RATIO
IN ISSEC SYSTEMS
1MW/m²
APPM HELIUM/DPA
THICKNESS OF CARBON SHIELD (FULL DENSITY)-cm
Al
316SS
Mo
V
Nb
Ta
0
10
20
30
40
45

FIGURE 10

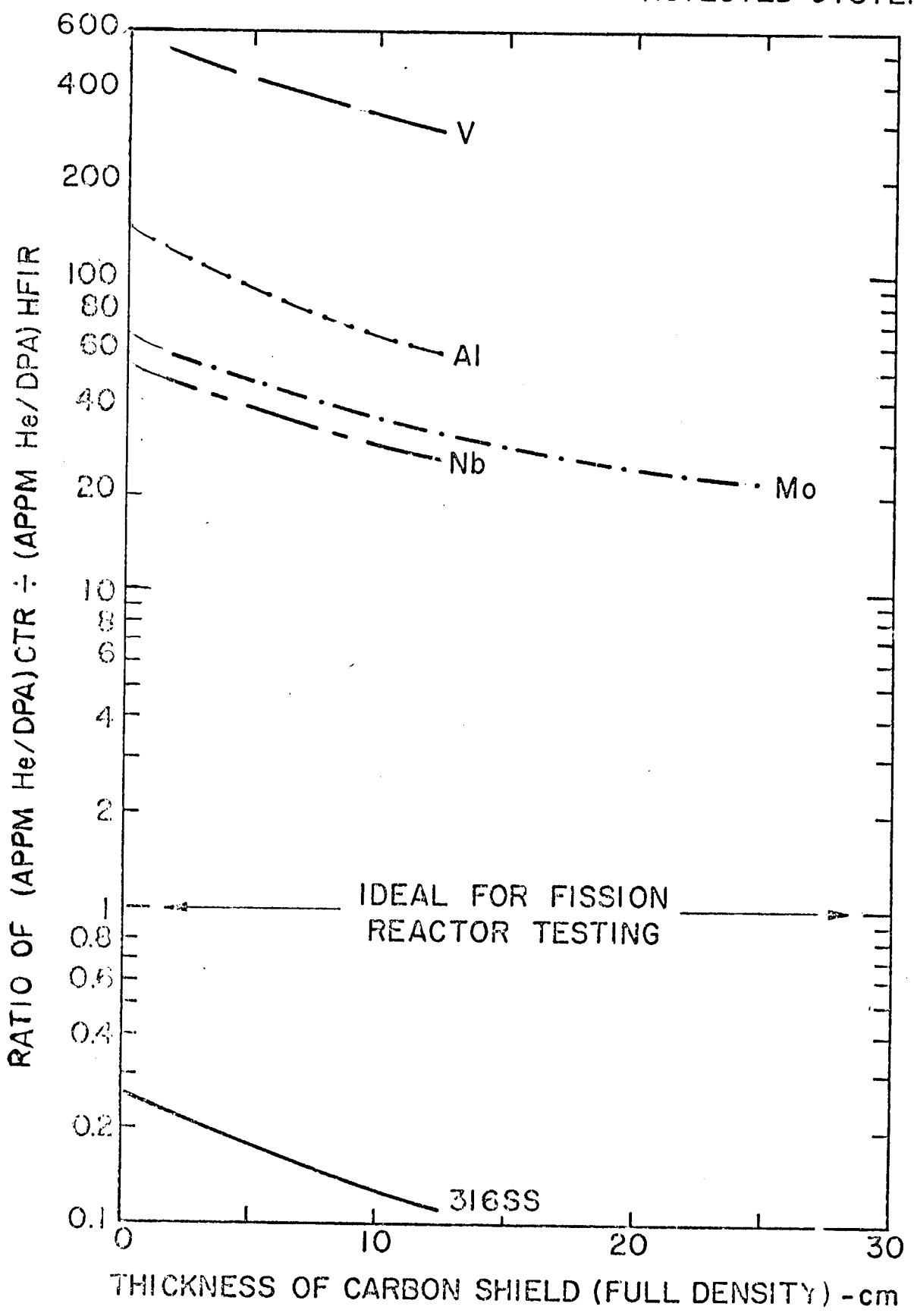
NORMALIZED He/DPA RATIOS FOR ISSEC PROTECTED SYSTEM
RATIO OF (APPM He/DPA) CTR ÷ (APPM He/DPA) HFIR
600
400
200
100
80
60
40
20
10
8
6
4
2
1
0.8
0.6
0.4
0.2
0.1
V
Al
Nb
Mo
IDEAL FOR FISSION
REACTOR TESTING
316SS
0
10
20
30
THICKNESS OF CARBON SHIELD (FULL DENSITY) - cm

Figure 11

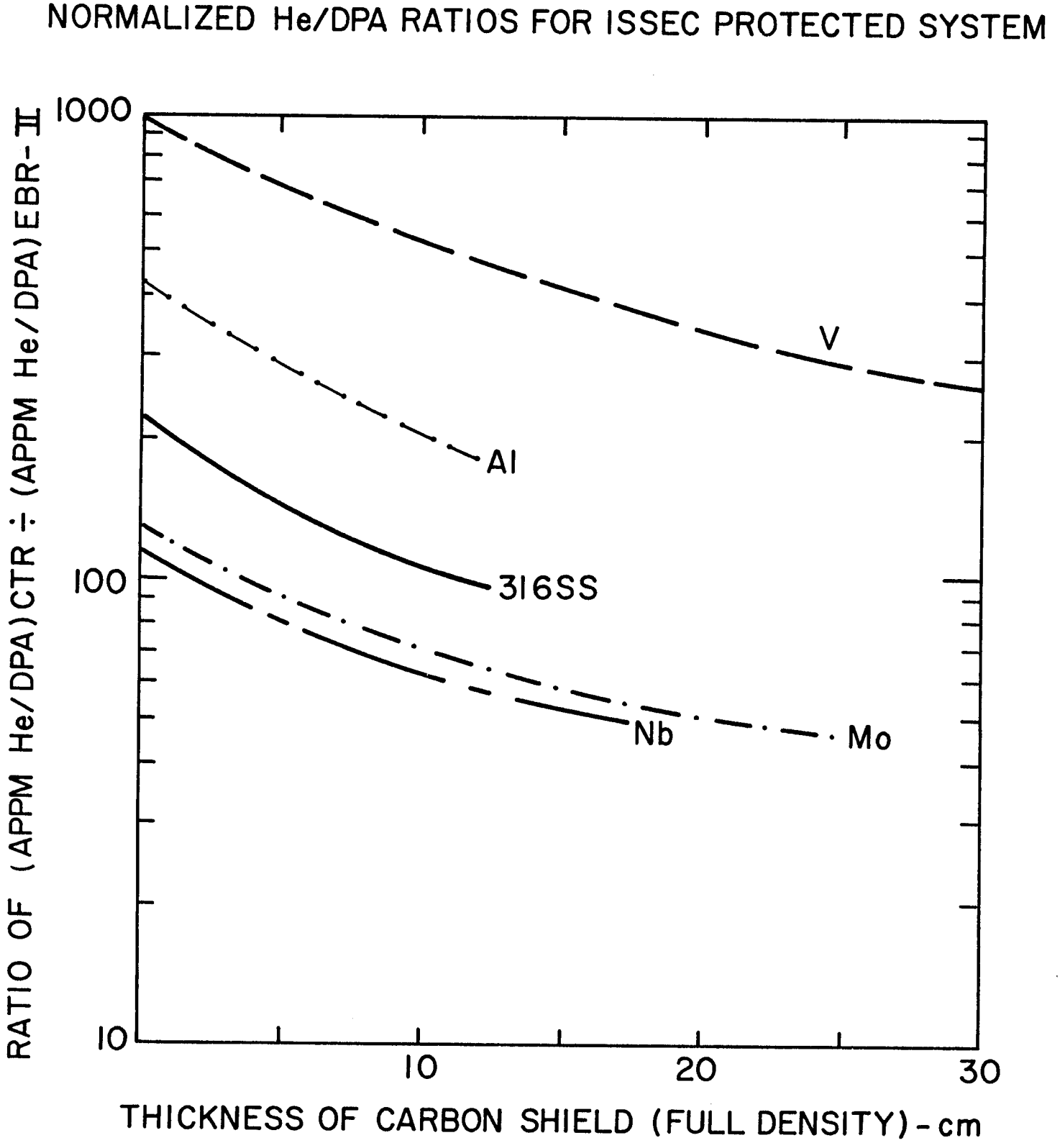
NORMALIZED He/DPA RATIOS FOR ISSEC PROTECTED SYSTEM
RATIO OF (APPM He/DPA)CTR ÷ (APPM He/DPA)EBR-II
1000
100
10
V
Al
316SS
Nb
Mo
10
20
30
THICKNESS OF CARBON SHIELD (FULL DENSITY) - cm

FIGURE 12

event of an accident. Unfortunately exactly the opposite conclusions can be drawn for V and Ta.

The reduction in long lived radioactivity for Al, V, and 316 SS can be viewed in three ways. First the total number of curies of long lived waste that need to be processed and stored is reduced. Secondly, the total mass of radioactive structure is reduced directly in proportion to the extension in wall life. Third, the density of long lived radioactive isotopes may be reduced or extended, depending on the product of the reduction in isotope production times the extension in wall life. Table 7 has been constructed to illustrate this last point and considers the cases for wall life limited by total dpa level and wall lives limited by total helium accumulation. It can be seen that the density of long lived radioisotopes is decreased from ~40 to 80% for 316 SS and Al respectively when the lifetime is limited by displacement damage only. If helium accumulation is the major factor then the radioisotope density can actually stay the same for Al and V or increase by 30% for 316 SS.

The magnitude of the long lived radioisotope density in Nb is actually increased by factors of 19-34 over the unprotected case while that of Ta is increased by a factor of 41 to 113. These increases are only partially compensated by the reduced volume of material (~factor of 10) that need be handled due to the extension of wall life time.

The reduction in metallic damage properties is partially taken up by increased radiation damage in the carbon. The most serious questions here are:

1.) Will any displacement damage survive at irradiation temperatures of 1500-2000°C ($0.5 - 0.66\ T/T_m$)?

2.) What will the generation of large amounts of He (several thousand appm) do to the carbon at high temperatures?

Table 7

Effect of 12.5 cm Carbon ISSEC on the Density (curies/cm^3) of Long Lived Radioisotopes at End of Life for Metallic Structural Component

	% Change in Density of Radioactivity Compared to Unprotected First Wall	
Material	dpa Lifetime Limit	Helium Gas Lifetime Limit
Al	-77	0
V	-48	0
316 SS	-41	+30
Nb	+1900	+3400
Ta	+4100	+11,300

Unfortunately there is no experimental evidence to answer these questions now but the authors tend to think that the displacement damage will anneal at these high temperatures but the helium may collect into bubbles causing dimensional instabilities. Obviously more work is needed here.

Conclusions

- The imposition of a 2000°C temperature maximum on the carbon ISSEC's will limit the full ISSEC thickness to ~6 cm and partial ISSEC's to ~30 cm at 1 MW/m^2 neutron wall loading and 10 $watts/cm^2$ surface heat load.
- The reduction of displacement damage and helium gas generation in metals is slightly greater for high Z as compared to low Z elements.
- Carbon ISSEC's can reduce the (appm He/dpa) ratios but they still will be 10-100 times higher than those found in current fission reactor facilities (except 316 SS).

Examples of the effectiveness of a 12.5 cm carbon ISSEC on damage parameters in Al, V, 316 SS, Nb, Mo and Ta are as follows:

- a reduction by a factor of 3-4 in the displacement rate
- a reduction by a factor of 6-14 in the helium gas production
- a reduction by a factor of 7-11 in the hydrogen gas production
- a reduction by a factor of 3-6 in the short lived radioactivity density in Al, Nb, and 316 SS
- an increase in the short term radioactivity density in Ta and V by a factor of 2 to 2.5
- a decrease in the long term radioactivity density in V, 316 SS and Al by a factor of 6-16
- an increase in the long term radioactivity density in Nb and Ta by a factor of 4-8 respectively.

There are two major unknown factors in the ISSEC concept which need experimental investigation:

- The effect of high dpa levels (~10-30) in carbon at temperatures of 1200-2000°C.
- The effect of high internal helium contents (3000-10000 appm) on the dimensional and mechanical properties of carbon at 1200-2000°C.

References

1. G. L. Kulcinski, R. W. Conn and G. Lang, Nucl. Fusion (to be published).

2. R. W. Conn, G. L. Kulcinski, H. Avci and M. El-Maghrabi, Nuclear Technology, 26, 125, 1975.

3. W. W. Engle, Jr., "A Users Manual for ANISN", K-1693, Oak Ridge Gaseous Diffusion Plant.

4. D. J. Dudziak, "Fusion Reactor Nuclear Analysis Methods and Applications", 8th Symp. on Fusion Technology, Noordijkerhout, The Netherlands, June 1974, p.

5. R. W. Wright et al., "SUPERTOG: A Program to Generate Fine Group Constants and Pn Scattering From ENDF/B", ORNL-TM-26 79, Oak Ridge National Laboratory (1969).

6. M. K. Drake, Ed., "Data Formats and Procedures for ENDF Neutron Cross Section Library", BNL-50279, Brookhaven National Laboratory (1970). See also O. Ozer and D. Garber "ENDF/B Summary Documentation" BNL-17541 and ENDF-201, Brookhaven National Laboratory (July 1973).

7. S. Pearlstein, private communication. See also S. Pearlstein, J. Nuclear Energy, 27, 81, (1973).

8. D. G. Doran, Nucl. Sci. Eng. 52, 398, 1973. See also Nucl. Sci. Eng. 49, 130, 1972.

9. G. L. Kulcinski, D. G. Doran, and M. A. Abdou, to be published, ASTM Proceedings of Radiation Effects on Structural Materials, Gatlinburg, Tenn., June 1974.

10. T. Y. Sung, Unpublished Work.

11. D. K. Sze, to be published, Trans. Am. Nucl. Soc., New Orleans Meeting, June 1975.

12. W. C. Morgan, J. Nuclear Energy, 51, 509, 1974.

13. W. J. Gray and W. C. Morgan, in Proc. 5th Symp. Engr. Problems of Fusion Research, p. 59, IEEE Pub. No. 73, CHO843-3-NPS (1974).

14. W. Bauer and G. J. Thomas, to be published, International Conf. on the Application of Ion Beams to Materials, Warwick England, September 1975.

15. D. G. Doran, G. R. Odette and N. J. Graves, p. 2 in Hanford Engineering Development Laboratory Report, HEDL-TME-75-24, February 1975.

Acknowledgement

Research was partially supported by the Energy Research and Development Administration and the Wisconsin Electric Utilities Research Foundation.

The authors wish to thank Mrs. Shirley Sze for her assistance in preparing the figures for this report.

Appendix A

46 Group Displacement Cross Sections - barns

Group	316 SS	Mo	Nb	V	Al	C
1	2225	1751	1717	2279	1924	1254
2	2078	1670	1613	2169	1909	1378
3	1993	1557	1518	2097	1883	1364
4	1955	1461	1435	2056	1823	1015
5	1913	1362	1372	2009	1733	1107
6	1903	1281	1305	1973	1710	1038
7	1898	1254	1238	1938	1710	1704
8	1848	1156	1165	1899	1695	789
9	1763	1108	1088	1861	1568	966.5
10	1703	1048	1010	1816	1703	829.7
11	1660	965	935	1752	1658	914.7
12	1623	916.2	863	1690	1620	1047
13	1560	887	797	1626	1549	1512
14	1493	843.2	737	1566	1568	1519
15	1410	780	683	1502	1538	1855
16	1375	759	637	1457	1500	1101
17	1295	741.1	610	1379	1474	1428
18	1275	711.9	610	1346	1556	844.6
19	1070	639.2	569	1073	1379	867.8
20	788	534.6	500	967.1	1211	915.5
21	634.4	442.1	461.6	849.8	1068	985.4
22	462.8	378.4	425.8	581.6	1023	1013
23	398.3	342.6	373.5	463.2	860.8	997.1
24	373	287.3	256	387.9	831.4	941.9
25	301.4	247.6	173.7	382.2	601.5	863
26	195.6	201.2	138.5	309.4	511.8	763
27	196.8	164.8	109.6	285.8	545.6	647
28	180.3	128.9	87.3	285.8	597.4	560
29	120.8	93.5	68.1	190.6	330.7	547
30	68.6	44.5	34.3	109	136.9	358

Group	316 SS	Mo	Nb	V	Al	C
31	93.1	20.1	17.6	212.6	231.5	193.5
32	26.3	13.8	9.3	106.3	132.1	99.4
33	15.8	6.7	5.2	146.5	97.4	49.5
34	5.2	3.6	1.9	8.44	32.5	24.6
35	3.56	2.2	1.5	.51	14.7	12.0
36	1.04	1.9	1.3	.26	6.3	5.8
37	.13	1.1	1.3	.36	2.3	2.8
38	.19	2.0	1.3	.36	.64	1.4
39	.27	8.0	1.3	.37	.88	0
40	.4	1.4	1.1	.54	1.11	0
41	.58	.41	.045	.78	1.41	0
42	.84	.19	.065	1.1	2.7	0
43	1.2	.23	.095	1.65	3.8	0
44	1.79	.33	.14	2.4	4.5	0
45	2.6	.48	0.2	3.5	8.3	0
46	5.3	1.0	0.4	6.83	14.6	0

The above 46 group displacement cross sections for 316SS, Mo, Nb, V, and Al are condensed from the 100 group cross sections given in references 8 and 9. The displacement threshold energies used are 24, 37, 36, 24 and 16 eV for 316 SS, Mo, Nb, V, and Al, respectively. In reference 9 , the secondary displacement function used is:

$$\nu(T) = \beta \frac{L(\varepsilon)}{\varepsilon} \frac{T}{2E_d}$$

where E_d is the effective displacement energy, taken to be 5/3 times displacement threshold energy,

$\varepsilon = A_L T$ and for pure materials of atomic number Z and atomic weight A,

$$A_L = \frac{0.01151}{(Z)^{7/3}} \quad eV^{-1}$$

$$L(\varepsilon) = \frac{\varepsilon}{[1 + K_L g(\varepsilon)]}$$

where $g(\varepsilon) = \varepsilon + 0.40244\ \varepsilon^{3/4} + 3.4008\ \varepsilon^{1/6}$

and $K_L = \frac{0.1334\ (Z)^{2/3}}{A^{1/2}}$

$\beta \simeq 0.8$

The carbon displacement cross sections are from W. C. Morgan, ref. 12 .

Appendix B

Reactions considered for radioactivity calculations

			Branching ratio	Half life
1.)	Niobium			
	$Nb^{93}(n,\alpha)$	Y^{90m}	.9	3.19 h
		Y^{90}	.1	64.0 h
	$Nb^{93}(n,\gamma)$	Nb^{94m}	.9	6.26 m
		Nb^{94}	.1	2.0×10^4 y
	$Nb^{93}(n,2n)$	Nb^{92m}	.667	10.13 d
		Nb^{92}	.337	stable
2.)	Vanadium			
	$V^{51}(n,\alpha)\ Sc^{48}$			1.82 d
	$V^{51}(n,\gamma)\ V^{52}$			3.75 m
	$V^{51}(n,p)\ Ti^{51}$			5.76 m
3.)	Aluminum			
	$Al^{27}(n,\alpha)\ Na^{24}$			15.0 h
	$Al^{27}(n,\gamma)\ Al^{28}$			2.27 m
	$Al^{27}(n,p)\ Mb^{27}$			9.5 m
	$Al^{27}(n,2n)$	Al^{26m}	.5	64 s
		Al^{26}	.5	7.4×10^5 y
4.)	Tantalum			
	$Ta^{181}(n,\alpha)$	Lu^{178m}	.5	20 m
		Lu^{178}	.5	30 m
	$Ta^{181}(n,\gamma)$	$Ta^{182\ m}$	.5	15.9 m
		Ta^{182}	.5	115 d
	$Ta^{181}(n,2n)$	Ta^{180m}		8.13 h

Appendix C

The Composition of 316 SS Used for These Radioactivity Calculations

Isotope	Atom Density (cm^{-3})
Si 28	1.566 E21
Si 29	7.980 E19
Si 30	5.250 E19
Cr 50	6.719 E20
Cr 52	1.306 E22
Cr 53	1.489 E21
Cr 54	3.719 E20
Mn 55	1.736 E21
Fe 54	3.249 E21
Fe 56	5.116 E22
Fe 57	1.223 E21
Fe 58	1.842 E20
Ni 58	6.615 E21
Ni 60	2.557 E21
Ni 61	1.160 E20
Ni 62	3.569 E20
Ni 64	1.053 E20

Appendix D

46 Group Neutron Fluxes at the First Mesh Point in the First Wall

Normalized to 10^{15} n's/cm^2 sec Incident 14.1 MeV Neutrons

Group #	TANTALUM FIRST WALL		316 SS FIRST WALL	
	No Graphite	12.5 cm Graphite	No Graphite	12.5 cm Graphite
1	2.3095 + 15*	1.4213 +14	2.3259 + 15*	1.4262 + 14
2	6.8326 + 13	5.2152 + 13	1.1157 + 14	5.3754 + 13
3	5.9694 + 13	3.1647 + 13	7.1843 + 13	3.2674 + 13
4	5.8469 + 13	2.5311 + 13	7.1850 + 13	2.6311 + 13
5	2.9480 + 13	1.3393 + 13	4.5608 + 13	1.4463 + 13
6	5.1643 + 13	3.5389 + 13	6.2184 + 13	3.63 + 13
7	5.7769 + 13	2.7592 + 13	6.5990 + 13	2.8585 + 13
8	3.2529 + 13	3.5714 + 13	4.1854 + 13	3.708 + 13
9	2.6626 + 13	2.0687 + 13	3.2631 + 13	2.202 + 13
10	3.3195 + 13	2.8799 + 13	3.9763 + 13	3.0527 + 13
11	2.9583 + 13	2.2629 + 13	3.4660 + 13	2.4321 + 13
12	3.3247 + 13	2.4197 + 13	3.7632 + 13	2.619 + 13
13	3.5168 + 13	2.1691 + 13	3.7388 + 13	2.373 + 13
14	3.8280 + 13	1.8710 + 13	3.8695 + 13	2.0927 + 13
15	4.1608 + 13	1.6028 + 13	3.8637 + 13	1.7992 + 13
16	5.1960 + 13	2.2917 + 13	4.6361 + 13	2.5186 + 13
17	6.0040 + 13	2.2859 + 13	5.3827 + 13	2.5719 + 13
18	7.5623 + 13	3.3726 + 13	7.3905 + 13	3.7625 + 13
19	2.7858 + 14	1.1479 + 14	2.6462 + 14	1.2979 + 14
20	3.4772 + 14	1.2656 + 14	3.1852 + 14	1.4280 + 14
21	4.1144 + 14	1.3103 + 14	3.3476 + 14	1.4062 + 14
22	4.5313 + 14	1.3215 + 14	3.3286 + 14	1.3157 + 14
23	4.8257 + 14	1.3258 + 14	3.1759 + 14	1.2470 + 14

Group #	TANTALUM FIRST WALL		316 SS FIRST WALL	
	No Graphite	12.5 cm Graphite	No Graphite	12.5 cm Graphite
24	4.7632 + 14	1.2920 + 14	2.6452 + 14	1.1129 + 14
25	4.3532 + 14	1.2206 + 14	2.5470 + 14	1.0689 + 14
26	3.7406 + 14	1.1272 + 14	1.9964 + 14	9.5222 + 13
27	3.0917 + 14	1.0287 + 14	1.5899 + 14	8.6641 + 13
28	2.5028 + 14	9.4072 + 13	1.3552 + 14	8.2045 + 13
29	3.2618 + 14	1.5910 + 14	1.6988 + 14	1.4102 + 14
30	1.9532 + 14	1.5704 + 14	9.8588 + 13	1.4172 + 14
31	7.5597 + 13	1.2386 + 14	5.0216 + 13	1.3015 + 14
32	2.3500 + 13	9.8327 + 13	2.3768 + 13	1.1606 + 14
33	5.6759 + 12	7.8128 + 13	1.0200 + 13	1.0957 + 14
34	9.7286 + 11	6.0633 + 13	2.8255 + 12	9.2084 + 13
35	1.3887 + 11	4.5953 + 13	6.4045 + 11	7.9846 + 13
36	2.6973 + 10	3.6149 + 13	1.5887 + 11	7.4086 + 13
37	3.5989 + 09	2.7618 + 13	3.8813 + 10	6.9059 + 13
38	1.6609 + 08	1.9332 + 13	9.1479 + 09	6.4237 + 13
39	2.4209 + 07	1.4961 + 13	2.4159 + 09	5.9756 + 13
40	6.6402 + 06	1.0273 + 13	3.4589 + 08	5.5683 + 13
41	1.0000 + 06	7.9146 + 12	3.1950 + 07	5.1885 + 13
42	2.3230 + 02	1.3862 + 12	9.4679 + 06	4.8350 + 13
43	7.2199 + 01	1.6099 + 13	1.7284 + 06	4.5004 + 13
44	3.8113 + 01	2.0265 + 13	2.0956 + 05	4.173 + 13
45	2.5257 + 01	1.9336 + 13	2.4277 + 04	3.5806 + 13
46	2.5756 + 01	1.9787 + 14	2.2899 + 03	4.6434 + 14

*Numbers in this table should be read as $a\pm n = ax10^{\pm n}$

Appendix E

It has been known for some time that anomalous helium production occurs in Ni because of $^{58}Ni(n,\gamma)$ $^{59}Ni(n,\alpha)$ reaction sequence. Therefore, calculations were performed to test how important the ^{59}Ni reaction is to helium production in 316 SS first wall with the comparatively softer spectrum characteristic of 12.5 cm of ISSEC. Ignoring the burnout of ^{58}Ni atoms, the number of ^{59}Ni atoms as a function of time, N^{59}, due to a concentration N^{58} of ^{58}Ni atoms undergoing (n,γ) reaction with a cross section σ^{γ}, is

$$N^{59}(t) = \sum_i N^{58}\sigma_i^{\gamma}\phi_i t \quad ,$$

where ϕ_i is the neutron flux in the i^{th} energy group. The number of helium atoms, N^{He}, produced in time, T, is then

$$N^{He} = \int_o^T \sum_j N^{59}(t)\sigma_j^{\alpha}\phi_j \, dt$$

$$= \frac{N^{58}T^2}{2} \sum_j \sum_i \sigma_i^{\gamma}\sigma_j^{\alpha}\phi_i\phi_j$$

where σ^{α} is the (n,α) cross section for ^{59}Ni. A more precise treatment would show that as the ^{59}Ni concentration reached steady state, N^{He} would be proportional to T, rather than T^2, which means the results presented here will give a pessimistic estimate of helium production. The results are shown in the following table. The (n,α) cross sections of Kirouac (Nucl. Sci. Eng., 46, 427, 1971) was used.

Table E-1

Additional helium generated as a result of $^{58}Ni(n,\gamma)$ $^{59}Ni(n,\alpha)$ reaction sequence in 316 SS

Operation Time (year)	appm He per 1 MW/m^2 wall loading	
	12.5 ISSEC	No ISSEC
1	1.14	.0023
2	4.55	.0094
5	28.45	.059
10	113.80	.23
20	455.19	.94

It is noted that the 1.14 appm He yr^{-1} from the Ni-59 reactions will be small compared to 280 appm He yr^{-1} generated by threshold reactions. Even after 20 years of operating time, the 455 appm He will be small (~8%) compared to the accumulated 5600 appm He due to the threshold reactions.

Appendix F

Table F-1 Neutron 46 Energy Group Structure in eV

Group	Group Limits E(Top)	E(Low)	E(Mid-Point)
1	1.4918 (+7)	1.3499 (+7)	1.4208 (+7)
2	1.3499 (+7)	1.2214 (+7)	1.2856 (+7)
3	1.2214 (+7)	1.1052 (+7)	1.1633 (+7)
4	1.1052 (+7)	1.0000 (+7)	1.0526 (+7)
5	1.0000 (+7)	9.0484 (+6)	9.5242 (+6)
6	9.0484 (+6)	8.1873 (+6)	8.6178 (+6)
7	8.1873 (+6)	7.4082 (+6)	7.7977 (+6)
8	7.4082 (+6)	6.7032 (+6)	7.0557 (+6)
9	6.7032 (+6)	6.0653 (+6)	6.3843 (+6)
10	6.0653 (+6)	5.4881 (+6)	5.7767 (+6)
11	5.4881 (+6)	4.9659 (+6)	5.2270 (+6)
12	4.9659 (+6)	4.4933 (+6)	4.7296 (+6)
13	4.4933 (+6)	4.0657 (+6)	4.2795 (+6)
14	4.0657 (+6)	3.6788 (+6)	3.8722 (+6)
15	3.6788 (+6)	3.3287 (+6)	3.5038 (+6)
16	3.3287 (+6)	3.0119 (+6)	3.1703 (+6)
17	3.0119 (+6)	2.7253 (+6)	2.8686 (+6)
18	2.7253 (+6)	2.4660 (+6)	2.5956 (+6)
19	2.4660 (+6)	1.8268 (+6)	2.1464 (+6)
20	1.8268 (+6)	1.3534 (+6)	1.5901 (+6)
21	1.3534 (+6)	1.0026 (+6)	1.1780 (+6)
22	1.0026 (+6)	7.4274 (+5)	8.726 (+5)
23	7.4274 (+5)	5.5023 (+5)	6.4649 (+5)
24	5.5023 (+5)	4.0762 (+5)	4.7893 (+5)
25	4.0762 (+5)	3.0197 (+5)	3.5480 (+5)
26	3.0197 (+5)	2.2371 (+5)	2.6284 (+5)
27	2.2371 (+5)	1.6573 (+5)	1.9472 (+5)
28	1.6573 (+5)	1.2277 (+5)	1.4425 (+5)
29	1.2277 (+5)	6.7379 (+4)	9.508 (+4)
30	6.7379 (+4)	3.1828 (+4)	4.9604 (+4)

Table F-1 (cont.)

Group	Group Limits E(Top)	E(Low)	E(Mid-Point)
31	3.1828 (+4)	1.5034 (+4)	2.3431 (+4)
32	1.5034 (+4)	7.1017 (+3)	1.1068 (+4)
33	7.1017 (+3)	3.3546 (+3)	5.2281 (+3)
34	3.3546 (+3)	1.5846 (+3)	2.4696 (+3)
35	1.5846 (+3)	7.4852 (+2)	1.1666 (+3)
36	7.4852 (+2)	3.5358 (+2)	5.5105 (+2)
37	3.5358 (+2)	1.6702 (+2)	2.6030 (+2)
38	1.6702 (+2)	7.8893 (+1)	1.2296 (+2)
39	7.8893 (+1)	3.7267 (+1)	5.8080 (+1)
40	3.7267 (+1)	1.7603 (+1)	2.7435 (+1)
41	1.7603 (+1)	8.3153 (+0)	1.2959 (+1)
42	8.3153 (+0)	3.9279 (+0)	6.1216 (+0)
43	3.9279 (+0)	1.8554 (+0)	2.8917 (+0)
44	1.8554 (+0)	8.7643 (-1)	1.3659 (+0)
45	8.7643 (-1)	4.1399 (-1)	6.4521 (-1)
46	4.1399 (-1)	2.2000 (-2)	2.1800 (-1)